Qualitative and quantitative analysis of tensegrity domes

Paulina OBARA, Maryna SOLOVEI[ID]***, and Justyna TOMASIK**[ID]

Faculty of Civil Engineering and Architecture, Kielce University of Technology, Poland

Abstract. The paper concerns steel domes with regard to the special structures named tensegrity. Tensegrities are characterized by the occurrence of self-stress states. Some of them are also characterized by the presence of infinitesimal mechanisms. The aim of this paper is to prove that only tensegrity domes with mechanisms are sensitive to the change of the level of initial prestress. Two tensegrity domes are considered. In addition, a standard single-layer dome is taken into account for comparison. The analysis is carried out in two stages. Firstly, the presence of the characteristic tensegrity features is examined (qualitative analysis). Next, the behavior under static external loads is studied (quantitative analysis). In particular, the influence of the initial prestress level on displacements, effort, and stiffness of the structure is analyzed. To evaluate this behavior, a geometrically non-linear model is used. The model is implemented in an original program written in the Mathematica environment. The analysis demonstrates that for a dome with mechanisms, the adjustment of pre-stressing forces influences the static properties. It has been found that the stiffness depends not only on the geometry and properties of the material but also on the initial prestress level and external load. In the case of the non-existence of mechanisms, structures are insensitive to the initial prestress level.

Key words: tensegrity dome; self-stress state; infinitesimal mechanism; geometrical non-linear analysis.

1. INTRODUCTION

Domes are one of the oldest covers used in civil engineering. These structures have been known since 27 BCE, i.e., since the Romans used stone blows to cover their palaces. In modern times, concrete or steel is used to build domes. The most popular ones are steel domes, which are lighter than other conventional forms. This kind of structure is the best solution for long-span roofs. Steel domes can be divided into standard (traditional) and non-standard ones.

The standard domes are built with rods assembled in single-layer or double-layer grids. There are also ribbed domes. Depending on the arrangement of the rods, the structures can be divided into several groups (dome patterns), i.e., Kiewit domes, Lamella domes, Schwedler domes, and others. The research on standard steel domes concerns increasing the load capacity of the structure of the load-bearing capacity of the structure [1] and methods of taking into account the impact of non-uniform loads [2–6] or imperfections [7–9]. Most of the research focuses on optimization design [10, 11], stability analysis [12, 13], and reliability analysis [14, 15].

The non-standard solutions are cable domes, which are structurally effective in long-span roofs. There are special cable structures named tensegrity. Tensegrity is composed of compressed elements (struts or rods) separated from each other and floating inside of the continuous net of tensed elements (cables). Although these systems are rod-like structures, some specific mechanical and mathematical properties distinguish them

from conventional cable domes. The components are in a self-equilibrated system of internal forces (self-stress state), which means that there is an equilibrium stress state among struts and cables under zero external loads. Self-stress states stabilize infinitesimal mechanisms, the occurrence of which is another immanent feature of tensegrity structures. In the absence of self-stress, tensegrity structures are geometrically variable. Stabilization occurs only after introducing the initial stresses. The first tensegrity dome was proposed and patented in 1988 by Geiger [16]. This type of roof has low-profile configurations that reduce wind lift and uneven snow settling, and use less material to cover the roof. One of the main advantages of this structure is that its weight per square meter does not change with increasing span. This solution was used on the roof of the Olympic Gymnastics Hall in Seoul. The Seoul gymnastics stadium dome was 118 m in diameter, and 15 m high. After the appearance of the Geiger dome, many researchers presented their ideas of cable structures, i.e., Wang [17], Rębielak [18], Kawaguchi [19], and Levy [20, 21]. Levy's idea was applied to the roof structure of Georgia Dome, the Atlanta Stadium in the USA. It is the largest dome in the world.

The most dominant subject in the literature, starting from the beginning of the idea of tensegrity to the present day, is the search for the geometrical configuration (the form-finding) of tensegrity structures. In recent years, the form-finding of cable domes was investigated by many authors as well [22–24]. Popular areas of research on tensegrity domes include structure optimization [25, 26] and the investigation of static and dynamic properties [27–29]. Nevertheless, there is a gap in the parametric analysis of tensegrity domes. This analysis provides the determination of the static or dynamic parameters as the function of the prestress forces. It is a very important aspect due to the

---

possibility of controlling the stiffness of tensegrity structures by modifying the level of self-stress state [29–31].

This paper focuses on the complete static analysis of tensegrity domes. This approach contains a qualitative and quantitative assessment. There is no such complete examination in the literature known to the authors. Most articles only focus on one of these two analyses. This article examines the behavior of two various tensegrity domes, i.e., the Geiger dome and the Levy dome. The choice of these two structures is justified as they are often selected for the analysis of cable domes. In the years 1990 – 2022, according to Google Scholar, the appearance of the Geiger dome in different articles counts more than 10'000 and more than 18'000 of Levy's dome. However, the behavior of these domes has never been compared before. These structures vary not only in geometry. The most important difference is the presence or absence of infinitesimal mechanisms. In the literature, structures with and without mechanisms are referred to as tensegrities [32] but their behavior is distinct. To prove this, static parametric analysis was performed and the behavior of domes under external load is studied. Symmetrical and asymmetrical loads are taken into account. In particular, the influence of initial prestress level on displacements, effort and stiffness of the structures are analyzed. To measure the changes in rigidity, a dimensionless parameter, the so-called global stiffness parameter (*GSP*), is used. The *GSP* parameter expresses the ratio of two strain energies, measured at the minimum and the i-th level of self-stress. It should be noted that in the literature on tensegrity domes, there is no parameter characterizing the stiffness. Additionally, a standard single-layer dome is also analyzed for comparison.

The quantitative assessment was performed by nonlinear analysis. The geometrically non-linear model, implemented in an original program, written in the Mathematica environment, was used.

2. METHODS OF ANALYSIS

Tensegrity domes are n-element ($e = 1, 2, \ldots, n$) spatial trusses with m degrees of freedom $\mathbf{q} \, (\in \mathbb{R}^{m \times 1})$:

$$\mathbf{q} = \begin{bmatrix} q_1 & q_2 & \ldots & q_m \end{bmatrix}^T. \tag{1}$$

These systems consist of tensioned cables and compressed struts in a self-stress state. Each element is characterized by Young's modulus E_e, a cross-sectional area A_e and a length L_e. The mechanical properties of analyzed domes are described by the elasticity matrix $\mathbf{E} \, (\in \mathbb{R}^{n \times n})$:

$$\mathbf{E} = \mathrm{diag} \begin{bmatrix} \dfrac{E_1 A_1}{L_1} & \dfrac{E_2 A_2}{L_2} & \ldots & \dfrac{E_n A_n}{L_n} \end{bmatrix}, \tag{2}$$

and by three linearized equations, i.e.: compatibility, material properties and equilibrium with boundary conditions included:

$$\mathbf{\Delta} = \mathbf{B} \, \mathbf{q}, \quad \mathbf{S} = \mathbf{E} \mathbf{\Delta}, \quad \mathbf{B}^T \mathbf{S} = \mathbf{P}, \tag{3}$$

where $\mathbf{B} \, (\in \mathbb{R}^{n \times m})$ is compatibility matrix, $\mathbf{\Delta} \, (\in \mathbb{R}^{n \times 1})$ is extension vector, $\mathbf{S} (\in \mathbb{R}^{n \times 1})$ is internal longitudinal forces, $\mathbf{E} \, (\in \mathbb{R}^{n \times n})$ is elasticity matrix and $\mathbf{P} (\in \mathbb{R}^{m \times 1})$ is load vector.

The compatibility matrix $\mathbf{B}$ of analyzed structures can be determined directly or using the formalism of the finite element method [33]. The compatibility matrix determination algorithm was presented in [34], among others.

The complete analysis of tensegrity structures is a two-stage process. Qualitative assessment is the first step and quantitative assessment is the second.

2.1. Qualitative analysis

Qualitative analysis is required to identify the immanent features of tensegrity structures, such as infinitesimal mechanisms and self-stress states that stabilize these mechanisms. There are a lot of methods for qualitative analysis (form-finding methods). Starting from the beginnings of the idea of tensegrity, i.e., the 1960s, to the present day, the search for geometrical configuration is the most popular subject of papers. The most common methods were described in [35]. The methods often used include, e.g., the spectral analysis of linear stiffness matrix, the analytical solutions, the force density method, the dynamic relaxation, and the singular value decomposition (SVD) of the compatibility matrix $\mathbf{B}$ [29, 30, 34, 36]. The SVD method is considered due to its ease of application and can be used both for simple and more complex structures. In the Mathematica environment, based only on the information of the compatibility matrix $\mathbf{B}$ the self-stress states and infinitesimal mechanisms can be determined using the command $\{\mathbf{Y}, \mathbf{N}, \mathbf{X}\} = $ [SingularValueDecomposition[$\mathbf{B}$]]:

$$\mathbf{B} = \mathbf{Y} \, \mathbf{N} \, \mathbf{X}^T, \tag{4}$$

where $\mathbf{Y} \, (\in \mathbb{R}^{n \times n}) = \begin{bmatrix} y_1 & y_2 & \ldots & y_n \end{bmatrix}$ and $\mathbf{X} (\in \mathbb{R}^{m \times m}) = \begin{bmatrix} x_1 & x_2 & \ldots & x_m \end{bmatrix}$ are orthogonal matrices and $\mathbf{N} (\in \mathbb{R}^{n \times m})$ is a rectangular diagonal matrix. The orthogonal matrices $\mathbf{Y}$ and $\mathbf{X}$, as well as the matrix $\mathbf{N}$, are related to eigenvectors and eigenvalues of the following problems:

$$\left(\mathbf{B}^T \mathbf{B} - \lambda \mathbf{I} \right) \mathbf{x} = 0, \quad \left(\mathbf{B} \mathbf{B}^T - \mu \mathbf{I} \right) \mathbf{y} = 0. \tag{5}$$

The mechanism can be considered as the eigenvector $\mathbf{x}_i = \mathbf{q} \, (\lambda_i = 0)$ related to the zero eigenvalue $\lambda_i = 0$ of the matrix in equation $(5)_1$, if it exists. Respectively, the self-stress state is the eigenvector $\mathbf{y}_i = \mathbf{S} \, (\mu_i = 0)$ related to the zero eigenvalue $\mu_i = 0$ of the matrix in equation $(5)_2$, if any.

If the self-stress state is defined as $\mathbf{y}_i$, the geometric stiffness matrix $\mathbf{K}_G(\mathbf{S}) \, (\in \mathbb{R}^{m \times m})$ is built. The normal forces $\mathbf{S}$, are determined as a function of the initial prestress force S:

$$\mathbf{S} = \mathbf{y}_i S, \tag{6}$$

The complete solution of the eigenproblem is provided by the spectral analysis of the stiffness matrix taking into account the effect of self-equilibrated forces ($\mathbf{K}_L + \mathbf{K}_G(\mathbf{S})$). If all eigenvalues are positive, the identified mechanism is infinitesimal and the structure is stable. Zero eigenvalues are related to finite mechanisms, whereas a negative eigenvalue represents the instability of the structure.

2

Bull. Pol. Acad. Sci. Tech. Sci., vol. 71, no. 1, p. e144574, 2023

2.2. Quantitative analysis

The quantitative assessment is the second step of the analysis of tensegrity structures. It is the parametric analysis leading to the determination of the impact of the self-stress state (initial prestress) on the behavior of the structure under static load. To assess this behavior, a geometrically non-linear model (third-order theory) is used [29, 31, 37]:

$$[\mathbf{K}_L + \mathbf{K}_G(\mathbf{S}) + \mathbf{K}_{NL}(\mathbf{q})]\,\mathbf{q} = \mathbf{P}, \qquad (7)$$

where $\mathbf{K}_L$ is linear stiffness matrix, $\mathbf{K}_{NL}(\mathbf{q})$ is the non-linear displacement stiffness matrix. The explicit matrices forms can be found for example in [29, 31].

An original program written in the Mathematica environment was used to solve the system of nonlinear equations (7). As a result, operations have been simplified using the functions and commands implemented there. The Newton–Raphson method was used to solve the algebraic system of nonlinear equations. The program allows the user to freely define the geometry of the structure, material parameters and loads, and then identify the self-stress state and track the behavior of selected static and geometric parameters as a function of this state. Additionally, a geometrically quasi-linear model (second-order theory) is also used to determine the influence of non-linearity:

$$[\mathbf{K}_L + \mathbf{K}_G(\mathbf{S})]\,\mathbf{q} = \mathbf{P}. \qquad (8)$$

The quantitative analysis contains:

- The determination of the minimum initial prestress level $S_{\min}$, which corresponds to the lowest level of prestress ensuring appropriate identification of the type of elements,
- The determination of the maximum initial prestress level $S_{\max}$, which depends on the load-bearing capacity of the most stressed elements,
- The assessment of the influence of the initial prestress level on displacements $\mathbf{q}$,
- The assessment of the influence of the initial prestress level on the effort of the structure:

$$W_{\max} = N_{\max}/N_{Rd}, \qquad (9)$$

where $N_{\max}$ is the maximal normal force and N_{Rd} is the load-bearing capacity.

- The assessment of the influence of the initial prestress on the rigidity of the structure determined by the global stiffness parameter GSP:

$$GSP = \frac{\left[\mathbf{q}\,(S_{\min})^T\,\mathbf{K}_S\,(S_{\min})\,\mathbf{q}\,(S_{\min})\right]}{\left[\mathbf{q}\,(S_i)^T\,\mathbf{K}_S\,(S_i)\,\mathbf{q}\,(S_i)\right]}, \qquad (10)$$

where $\mathbf{K}_S(S_{\min})$ and $\mathbf{q}(S_{\min})$ are a secant stiffness matrix and a design displacement vector with a minimum initial prestress level, and $\mathbf{K}_S(S_i)$ and $\mathbf{q}(S_i)$ – at i-th prestress level.

3. EXAMPLES AND RESULTS

The article presents a parametric analysis of two non-standard domes (tensegrity), i.e., Geiger and Levy domes. For comparison, the standard single-layer dome with the Schwedler pattern is also considered. It is assumed that the cables in tensegrity domes are made of S460N steel. Type A cables with Young modulus 210 GPa [38] are used. The struts are made of a hot-finished circular hollow section (S355J2 steel) with the Young modulus 210 GPa. The profiles and the maximum load-bearing capacities of elements are described separately for each dome later in this chapter. The maximum length of domes is 20 m and the maximum height, measured from the level of the supports is 3.5 m. The structures are supported in all external nodes.

At first, the qualitative assessment of structures is carried out and the characteristic features are examined. The analysis can be performed by having only the knowledge of the geometry of the structures. The qualitative analysis is necessary for the correct assessment of the structure in the following step.

The quantitative assessment is performed as the next. The behavior under static external loads is studied. It is a parametric analysis in which the impact of the self-stress level on the displacements, effort and stiffness of the structures is examined.

3.1. Models of domes

The first structure to be analyzed is the modified Geiger dome with six load-bearing girders (Fig. 1a). The modification from the original Geiger's patent is to add additional horizontal cables. The structure consists of 73 elements, i.e., 13 struts (thick lines) and 60 cables (thin lines). The struts are designed as tubes CHS 127×5.6. Due to different lengths, the struts were divided into three groups, i.e., six struts of 3.83 m length, five struts of 2.33 m length and one strut of 1 m length, with the maximum load-bearing capacity of 418 kN, 640 kN and 741 kN, respectively. In turn, the cables are assumed to be made of "D42" with a maximum load-bearing capacity of 504.4 kN.
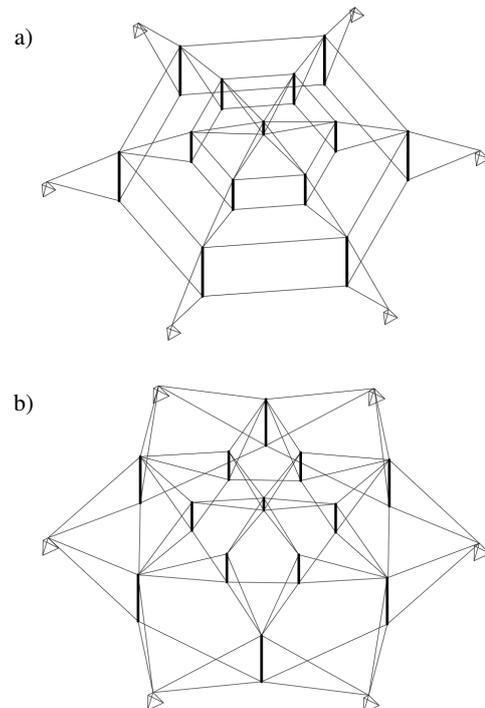
Fig. 1. Non-standard (tensegrity) domes: a) Geiger dome, b) Levy dome

Bull. Pol. Acad. Sci. Tech. Sci., vol. 71, no. 1, p. e144574, 2023

3

The second analyzed tensegrity structure is the original Levy dome (Fig. 1b). In Geiger's form, the ridge cables are radially oriented, so the roof is divided into many wedge-shaped basic units in the plan. To tension the membrane, some valley cables are also provided in each panel between ridge cables. However, in the Levy form, the ridge cables form a triangular pattern. The Levy dome consists of 85 elements, i.e., 13 struts (thick lines) and 72 cables (thin lines). The struts are designed as tubes CHS 108×4.5. The length of struts is the same as in the case of Geiger dome and the load-bearing capacity equals 224 kN, 402 kN and 499 kN, respectively. In turn, the cables are assumed to be made of "D36" with a maximum load-bearing capacity of 367.5 kN.

The single-layer steel standard structure with a popular type of network, introduced by Schwedler in 1863 (Fig. 2), is the last analyzed dome. This type of pattern was chosen due to its popular application in real objects. The most known are Bojangles Coliseum built in 1955 (100 m in diameter), Astrodome built in 1965 (220 m), Caesars Superdome built in 1975 (207 m), and National Stadium Singapore built in 2014 (312 m), which holds the record for the largest dome structure in the world. Schwedler dome consists of meridional rods connected by latitudinal ones with an additional diagonal member dividing each trapezium "mesh eye" into two triangles. Additional diagonal elements result in high resistance to unsymmetrical loads, significantly increase the reliability of the dome and reduce the sensitivity to node jumps.
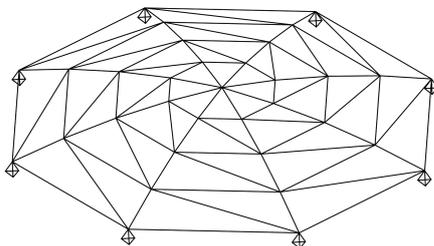
Fig. 2. Standard single-layer dome with Schwedler pattern

The analyzed dome consists of 88 rods divided into 3 groups, i.e., meridional (CHS 101.6x3.2), latitudinal (CHS 108x4) and diagonal (CHS 101.6x5) with a maximum length of 7.65 m, 2.55 m, and 7.12 m, respectively. The maximum load-bearing capacity equals 244 kN, 396 kN, and 216 kN, respectively.

3.2. Quanlitative analysis

The qualitative analysis leads to the identification of the self-stress states and infinitesimal mechanisms. Therefore, the geometrical and mechanical characteristics do not affect these properties, all constants were assumed as unitary, hence the elasticity matrix is a unit matrix $\mathbf{E} = \mathbf{I}$.

The results of the qualitative analysis are shown in Table 1. The considered domes have a comparable number of elements and nodes but a different number of struts. Additionally, domes differ in the number of identified mechanisms and self-stress states.

The modified Geiger dome (G) features eight mechanisms and three self-stress states. The modification, in relation to the

Table 1
Results of qualitative analysis

Dome type	Number of:					
	nodes	degrees of freedom	all elements	struts	self-stress states	mechanisms
Geiger	20	42	73	13	3	8
Levy	32	78	85	13	7	–
Single-layer	33	75	88	88	–	–

original Geiger's patent, leads to the reduction of the mechanisms and the increase in the number of self-stress states (the regular Geiger dome is characterized by 18 mechanisms and one self-stress state). The obtained self-stress states do not identify the type of elements properly. Only the superimposed self-stress state $\mathbf{y}_G$ is correct. In Fig. 3a, the values of self-equilibrium normal forces (6) are shown. The eigenvalues of the matrix $(\mathbf{K}_L + \mathbf{K}_G(\mathbf{S}))$ are positive, thus the identified mechanisms are infinitesimal and the structure is stable.

The Levy dome (L) is characterized by the lack of mechanism and the presence of seven self-stress states. As in the case of the Geiger dome, only the superposition of all states $\mathbf{y}_L$ identifies the type of elements properly. Figure 3b presents the values of self-equilibrium normal forces (6).

a)

—	1.739 S
—	0.227 S
—	0.756 S
—	0.236 S
—	2.006 S
—	0.801 S
—	0.220 S
—	0.306 S
—	-1.000 S
—	-0.265 S
—	-0.228 S

b)

—	1.739 S
—	1.003 S
—	0.461 S
—	0.368 S
—	0.511 S
—	0.870 S
—	-0.380 S
—	-1.000 S
—	-0.304 S
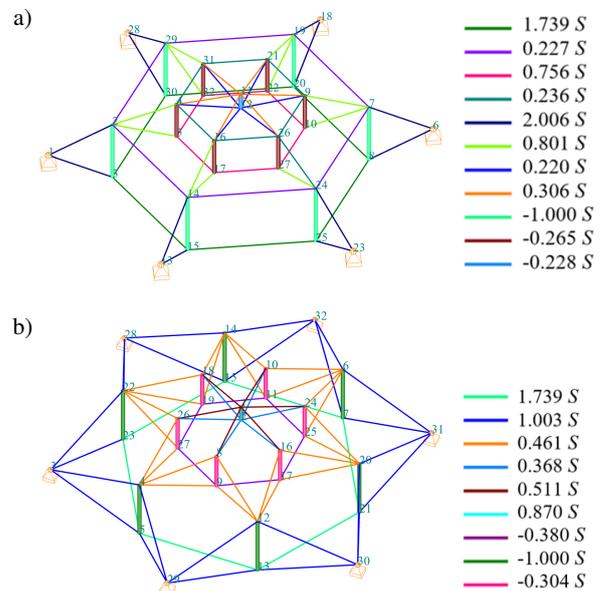
Fig. 3. Values of self-equilibrium normal forces (9): a) Geiger, b) Levy

The single-layer Schwedler dome (SL) is not characterized by tensegrity features such as infinitesimal mechanisms and self-stress states. This is a standard steel dome.

3.3. Quantitative analysis

In the quantitative analysis, the behavior of three domes (G, L, SL) is studied. Two variants of load are considered. In the first case, the load was applied symmetrically (Fig. 4a) (G1, L1,

4

Bull. Pol. Acad. Sci. Tech. Sci., vol. 71, no. 1, p. e144574, 2023

SL1), whereas in the second – asymmetrically (Fig. 4b) (G2, L2, SL2). In both cases, the vertical (z-direction) forces (P_z) and plane ones (P_{xy}) are assumed to be the nominal value of 1 kN ($P_x = P_y = 0.707$;kN). It is not a real load. The conducted considerations are intended only to compare and indicate the differences in the behavior of the analyzed domes.
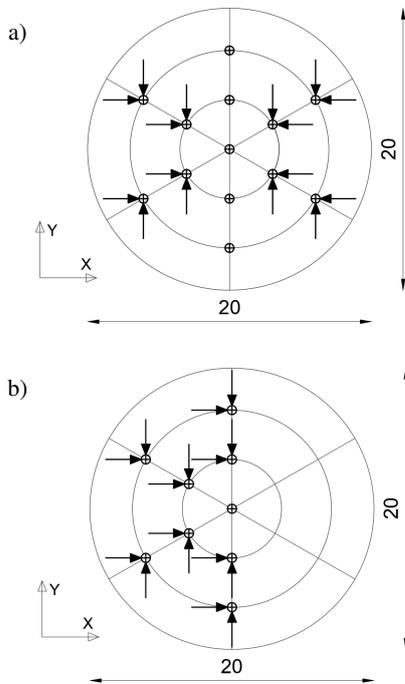
Fig. 4. Scheme of load: a) symmetrical (G1, L1, SL1), b) asymmetrical (G2, L2, SL2)

The calculation procedure includes the geometrically quasi-linear (II) and non-linear (III) analysis. Unlike the qualitative analysis, the results of the quantitative analysis depend on the materials and cross-sections of elements.

In the case of tensegrity, the quantitative assessment is a parametric analysis leading to the determination of the impact of initial prestress level on the behavior of the structures. The static and geometric parameters are the function of this state. The first step of analysis is the determination of a prestress range, which is an individual feature of the structure. The minimum prestress level (S_{min}) depends on the proper distribution of normal forces in the structure elements, i.e., tensile forces must be present in cables and compressive – in struts. In some cases, the external load causes a different distribution of normal forces, which can be corrected only by introducing an appropriate level of initial prestress. The minimum prestress level for the Geiger dome is equal to $S_{min} = 21$ kN, whereas for the Levy dome – $S_{min} = 11$ kN. In turn, the value of the maximum prestress level (S_{max}) depends on the load-bearing capacity of the most stressed elements. For both structures, it was assumed as $S_{max} = 190$ kN and then the maximum effort of structures is $W_{max} = 0.91$.

In the case of a single-layer dome, self-stress states do not exist, and the static and geometric parameters are constant. To compare the different behavior of the analyzed domes, the obtained results are shown in graphical form.

Firstly, the displacements of the upper middle node are presented (Figs. 5–7). In the case of the Levy dome, regardless of the load variant (symmetrical L1, asymmetrical L2), the displacements do not depend on the prestress level and they are constant. Additionally, the impact of non-linearity is insignificant (the results obtained from second order theory (II) and third order theory (III) are the same). This structure behaves like the single-layer dome. In turn, the behavior of Geiger dome is different. The displacement q_x (Fig. 5) and q_y (Fig. 6) depend on the level of the initial prestress and additionally on the load variant. The displacements decrease as the initial prestress increases.
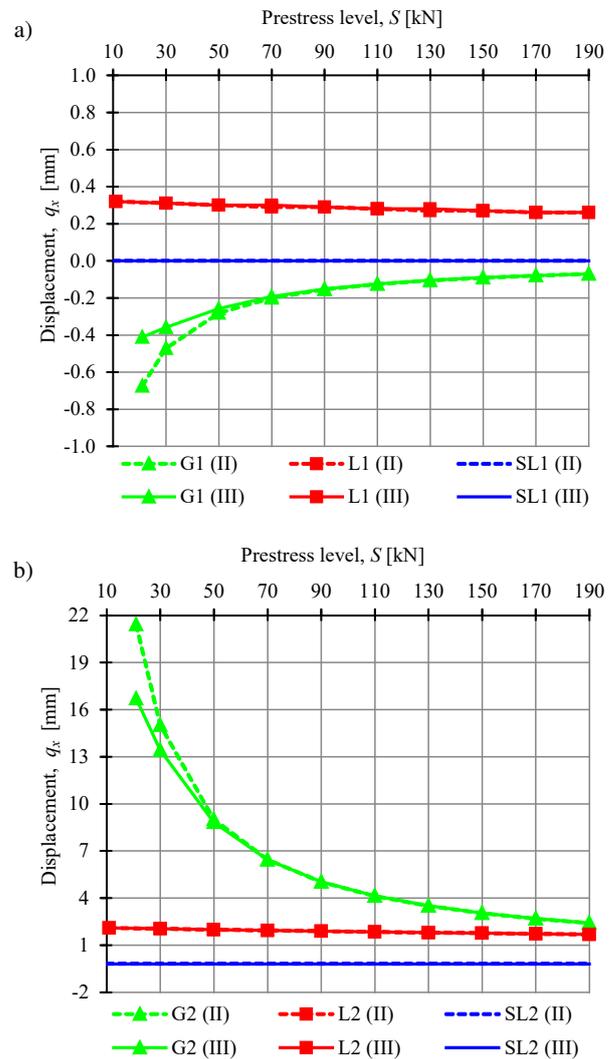
Fig. 5. Impact of the initial prestress level S on the displacement q_x for: a) symmetrical load, b) asymmetrical load

However, in the case of the asymmetrical load (G2), the displacements are higher than in the case of a symmetrical load (G1). This type of load causes displacements consistent with the infinitesimal mechanisms. The behavior of the displacement q_z varies (Fig. 7). According to the second-order theory, it is not

Bull. Pol. Acad. Sci. Tech. Sci., vol. 71, no. 1, p. e144574, 2023

5
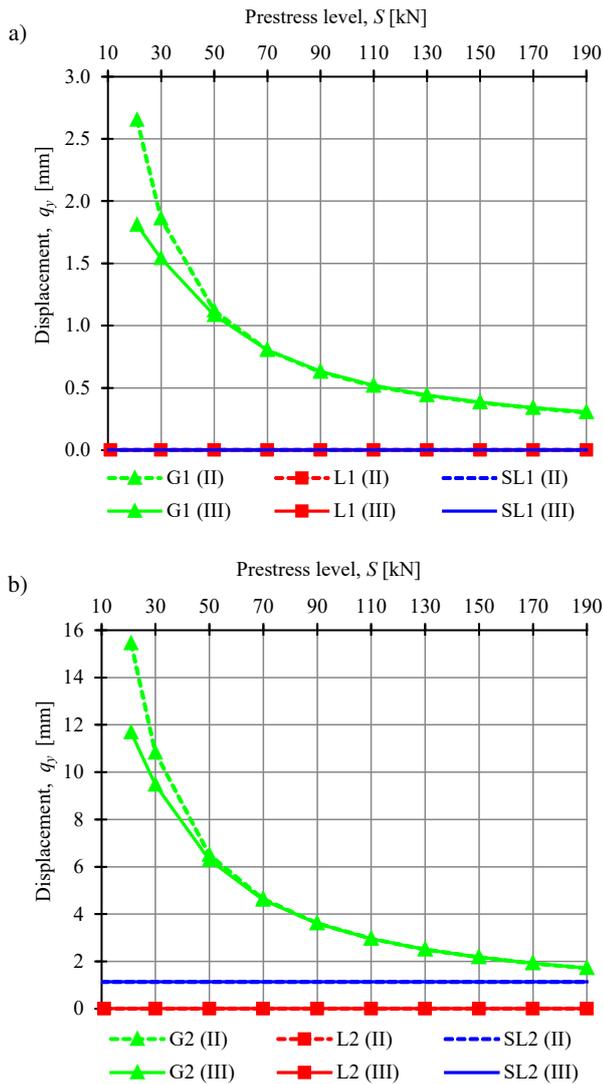
Fig. 6. Impact of the initial prestress level S on the displacement q_y for: a) symmetrical load, b) asymmetrical load

Fig. 7. Impact of the initial prestress level S on the displacement q_z for: a) symmetrical load, b) asymmetrical load

dependent on the level of initial prestress and is equal to almost zero (this displacement in all mechanisms is zero). Nonetheless, the calculations performed according to the third-order theory confirm that displacement is correlated with the level of initial prestress. Moreover, the initial prestress forces have a greater influence on the displacement with lower external loads. The conducted analyses show the influence of non-linearity is significant at low values of initial prestress forces. As prestressing forces increase, the differences between the calculations performed according to the second- and third-order theory become smaller. Although in the case of the assumed low load values, the results are similar. For the real load, the impact of nonlinearity is significant. For example, Fig. 8 shows the displacement q_x in the case of asymmetrical load $P_z = P_{xy} = 30$ kN. Moreover, the initial prestress forces have a greater influence on the displacements of the structure with lower external loads.

Next, the maximum effort of the structure (W_{max}) is calculated (Fig. 9a). For the Levy dome the increase of the effort is linear, whereas for the Geiger one – nonlinear. Due to the

Fig. 8. Impact of the initial prestress level S on the displacement q_x of Geiger dome in the case of asymmetrical load $P_z = P_{xy} = 30$ kN

6

Bull. Pol. Acad. Sci. Tech. Sci., vol. 71, no. 1, p. e144574, 2023

low load values, the non-linearity is not significant. To better describe the differences between a tensegrity dome with and without mechanisms, the global stiffness parameter (*GSP*) is calculated (Fig. 9b). For the first type of dome, the *GSP* increases with the prestress level. The almost linear relationship results in low load values (as in the case of $W_{\max}$). For the dome without mechanism, the *GSP* is constant (for the asymmetrical load – almost constant).
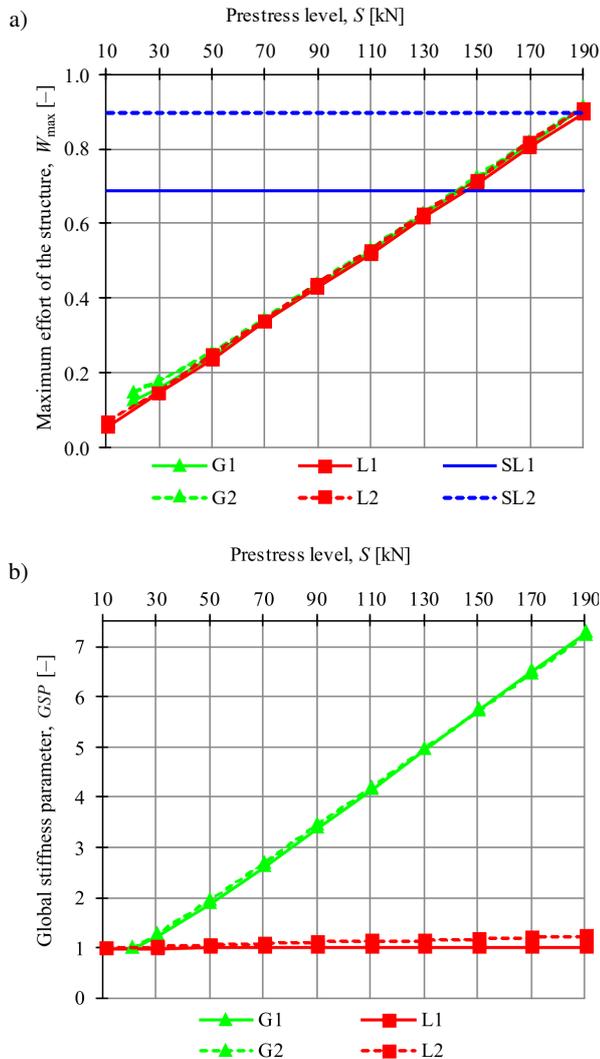
Fig. 9. Impact of the initial prestress level *S* on the: a) maximum effort of the structure $W_{\max}$, b) global stiffness parameter *GSP*

4. CONCLUSIONS

This paper aims to compare the behavior of tensegrity domes. The two most popular tensegrity domes, the Geiger dome and the Levy dome, are analyzed. It was found that the behavior of domes was different under the influence of external loads. The difference is related to the occurrence of an infinitesimal mechanism, i.e., only the Geiger dome is characterized by the infinitesimal mechanism. The paper focuses on the possibility of the active control of the stiffness of the tensegrity dome throughout the change of the level of self-stress.

The Geiger dome is characterized by the presence of both immanent features. The behavior of this structure can be controlled by the adjustment of the self-stress level. The stiffness depends not only on the geometry and material properties but also on the initial prestress level and external load. The impact of the load is the most significant at low values of the initial prestress forces. Additionally, the Geiger dome is more susceptible to asymmetrical load, which causes displacements consistent with infinitesimal mechanisms. In the case of a symmetrical load, the displacements are smaller. However, regardless of the type of load, the stiffness at the maximum prestress level increases more than seven times. Due to the influence of the external load on the stiffening of the structure, the analysis should be carried out assuming the hypothesis of large displacements. In turn, the Levy dome is characterized only by the self-stress states. In this case, the initial prestressing is possible, but this structure is insensitive to the changes in the force level. Prestressing increases only the effort of structures, but the stiffness is constant. The Levy dome behaves like a standard dome and the quantitative analysis can be carried out using a quasi-linear geometric model. The question then arises, what is the point of prestressing a structure? The introduction of the initial prestress is required only when the external load causes an incorrect distribution of normal forces in the elements of the structure. In that case, the minimum prestress level that corrects this distribution should be specified.

This paper focuses on the parametric analysis of real tensegrity domes. This area of research is still underdeveloped. The conducted research helps to better understand the mechanical properties of tensegrity systems. The comparative analysis, presented in this paper, gives two clear conclusions. On the one hand, the stiffness can be easily rectified by the change of the level of prestressing, and on the other, the prestressing of some structures does not make sense. The first conclusion refers to the domes characterized by the presence of infinitesimal mechanisms. In such structures, the control of the static parameters facilitates the adaptation to the required design parameters. These tensegrities offer many advantages and are a better alternative to the domes without mechanisms that can be only used as avant-garde architectural designs.

REFERENCES

[1] A. Zingoni and N. Enoma, "On strength and stability of elliptic toroidal domes," *Eng. Struct.*, vol. 207, p. 110241, 2020, doi: 10.1016/j.engstruct.2020.110241.

[2] S. Kato, J.M. Kim, and M.C. Cheong, "A new proportioning method for member sections of single-layer reticulated domes subjected to uniform and non-uniform loads," *Eng. Struct.*, vol. 25, no. 10, pp. 1265–1278, 2003, doi: 10.1016/S0141-0296 (03)00077-4.

[3] X. Zhao, S. Yan, and Y. Chen, "Comparison of progressive collapse resistance of single-layer latticed domes under different loadings," *J. Constr. Steel Res.*, vol. 129, pp. 204–214, 2017, doi: 10.1016/j.jcsr.2016.11.012.

[4] L. Tian, J. He, C. Zhang, and R. Bai, "Progressive collapse resistance of single-layer latticed domes subjected to non-uniform snow loads," *J. Constr. Steel Res.*, vol. 176, p. 106433, 2021, doi: 10.1016/j.jcsr.2020.106433.

[5] X. Yan, Y. Yang, Z. Chen, and Q. Ma, "Mechanical properties of a hybrid cable dome under non-uniform snow distribution," *J. Constr. Steel Res.*, vol. 153, pp. 519–532, 2019, doi: 10.1016/j.jcsr.2018.10.022.

[6] U. Radoń, P. Zabójszcza, and D. Opatowicz, "Assesment of the effect of wind load on the load capacity of a single-layer bar dome," *Buildings*, vol. 10, no. 179, pp. 1–27, 2020, doi: 10.3390/buildings10100179.

[7] H. Karimi and I.M. Kani, "Finding the worst imperfection pattern in shallow lattice domes using genetic algorithms," *J. Building Eng.*, vol. 23, pp. 107–113, 2019, doi: 10.1016/j.jobe.2019.01.018.

[8] J. Błachut, "Impact of local and global shape imperfections on buckling of externally pressurised domes," *nt. J. Pressure Vessels Pip.*, vol. 188, p. 104178, 2020, doi: 10.1016/j.ijpvp.2020.104178.

[9] P. Zabojszcza and U. Radoń, "The impact of node location imperfections on the reliability of single-layer steel domes," *Appl. Sci.*, vol. 9, no. 13, p. 2742, 2019, doi: 10.3390/app9132742.

[10] M. Lu and J. Ye, "Guided genetic algorithm for dome optimization against instability with discrete variables," *J. Constr. Steel Res.*, vol. 139, pp. 149–156, 2017, doi: 10.1016/j.jcsr.2017.09.019.

[11] M. Lu and J. Ye, "Design optimization of domes against instability considering joint stiffness," *J. Constr. Steel Res.*, vol. 169, p. 105757, 2020, doi: 10.1016/j.jcsr.2019.105757.

[12] G.P. Cimellaro and M. Domaneschi, "Stability analysis of different types of steel scaffolds," *Eng. Struct.*, vol. 152, pp. 535–548, 2017, doi: 10.1016/j.engstruct.2017.07.091.

[13] Y. Guan, L.N. Virgin, and D. Helm, "Structural behavior of shallow geodesic lattice domes," *Int. J. Solids Struct.*, vol. 155, pp. 225–239, 2018, doi: 10.1016/j.ijsolstr.2018.07.02.

[14] P. Zabojszcza, U. Radoń, and W. Szaniec, "Probabilistic approach to limit states of a steel dome," *Materials,* vol. 14, no. 19, p. 5528, 2021, doi: 10.3390/ma14195528.

[15] A. Dudzik and B. Potrzeszcz-Sut, "Hybrid approach to the first order reliability method in the reliability analysis of a spatial structure," *Appl. Sci.*, vol. 11, no. 2, p. 648, 2021, doi: 10.3390/app11020648.

[16] D.H. Geiger, "The design and construction of two cable domes for the Korea Olympics. Shells, Membranes and Space Frame," in *Proc. IASS Symposium*, Osaka, 1986, pp. 265–272.

[17] B.B. Wang, "Cable-Strut system: part 1, tensegrity," *J. Construct. Steel Res.*, vol. 45, no. 3, pp. 281–289, 1998.

[18] J. Rębielak, "Structural system of cable dome shaped by means of simple form of spatial hoops," in *Proc. Lightweight structures in Civil Engineering*, 2000, pp. 114–115.

[19] M. Kawaguchi, I. Tatemichi, and P.S. Chen, "Optimum shapes of a cable dome structure," *Eng. Struct.*, vol. 21, no. 8, pp. 719–725, 1999, doi: 10.1016/S0141-0296(98)00026-1.

[20] M. Levy and G. Castro, "Analysis of the Georgia dome Cable Roof," in *Proc. of the Eight Conference of Computing in Civil Eng. And Geogr. Inf. Systems Symposium, ASCE*, 1992, pp. 7–9.

[21] M. Levy, "Floating fabric over Georgia dome," *Civil Eng. ASCE*, vol. 61, no. 11, pp. 34–37, 1991.

[22] J. Lee, H.C. Tran, and K. Lee, "Advanced form-finding for cable dome structures," *in Proc. of IASS Symposium*, 2009.

[23] Y. Chen, Q. Sun, and J. Feng, "Group-theoretical form-finding of cable-strut structures based on irreducible representations for rigid-body translations," *Int. J. Mech. Sci.*, vol. 144, pp. 205–215, 2018, doi: 10.1016/j.ijmecsci.2018.05.057.

[24] Y. Xue, Y. Luo, and X. Xu, "Form-finding of cable-strut structures with given cable forces and strut lengths," *Mech. Res. Commun.*, vol. 106, p. 103530, 2020, doi: 10.1016/j.mechrescom.2020.103530.

[25] X. Yuan, L. Chen, and S. Dong, "Prestress design of cable domes with new forms," *Int. J. Solids Struct.*, vol. 44, pp. 2773–2782, 2007, doi: 10.1016/j.ijsolstr.2006.08.026.

[26] S. Krishnan, "Structural design and behavior of prestressed cable domes," *Eng. Struct.*, vol. 209, p. 110294, 2020, doi: 10.1016/j.engstruct.2020.110294.

[27] X. Shen, Q. Zhang, D.S.H. Lee, J. Cai, and J. Feng, "Static behavior of a retractable suspen-dome structure," *Symmetry*, vol. 13, no. 7, p. 1105, 2021, doi: 10.3390/sym13071105.

[28] G. Sun and S. Xiao, "Test and numerical investigation mechanical behavior of cable dome," *Int. J. of Steel Struct.*, vol. 21, no. 4, pp. 1502-1514, 2021, doi: 10.1007/s13296-021-00517-7.

[29] P. Obara, *Dynamic and dynamic stability of tensegrity structures*, Kielce: Wydawnictwo Politechniki Świętokrzyskiej, 2019. (in Polish)

[30] J. Kłosowska, P. Obara, and W. Gilewski, "Self-stress control of real civil engineering tensegrity structures," *AIP Conference Proceedings 1922*, 2018, p. 150004, doi: 10.1063/1.5019157.

[31] P. Obara and J. Tomasik, "Parametric analysis of tensegrity plate-like structure: Part 2 – Quantitative Analysis," *App. Sci.*, vol. 11, no. 2, p. 602, 2021, doi: 10.3390/app11020602.

[32] P. Obara, J. Kłosowska, and W. Gilewski, "Truth and myths about 2D tensegrity trusses," *App. Sci.*, vol. 9, p. 179, 2019, doi: 10.3390/app9010179.

[33] O.C. Zienkiewicz and R.L. Taylor, *The Finite Element Method. Vol. 1. The Basis*, London: Elsevier Butterworth-Heinemann, 2000.

[34] W. Gilewski *et al.*, "Application of singular value decomposition for qualitative analysis of truss and tensegrity structures," *Acta Sci. Pol. Hortorum Cultus*, vol. 11, no. 3, p. 14, 2015.

[35] A.G. Tibert and S. Pellegrino, "Review on Form-Finding methods for tensegrity Structures," *Int. J. Space Struct.*, vol. 18, no. 4, pp. 209–223, 2003, doi: 10.1260/026635103322987940.

[36] P. Obara and J. Tomasik, "Parametric analysis of tensegrity plate-like structure: Part 1 – Qualitative Analysis," *App. Sci.*, vol. 10, no. 20, pp. 7042, 2020, doi: 10.3390/app10207042.

[37] P. Obara and J. Tomasik, "Active control of stiffness of tensegrity plate-like structures built with simplex modules," *Materials*, vol. 14, no. 24, p. 7888, 2021, doi: 10.3390/ma14247888.

[38] Eurocode 3: Design of steel structures – Part 1–11: Design of structures with tension components, EN 1993-1-11: 2006.

8

Bull. Pol. Acad. Sci. Tech. Sci., vol. 71, no. 1, p. e144574, 2023